BRDF and gloss computation of polyurethane coatings from roughness measurements: Modelling and experimental validation

Benoît Wittmann, Pierre Montmitonnet, Alain Burr, Christian Gauthier, Jean-François Agassant, Alain Casoli

▶ **To cite this version:**

Benoît Wittmann, Pierre Montmitonnet, Alain Burr, Christian Gauthier, Jean-François Agassant, et al.. BRDF and gloss computation of polyurethane coatings from roughness measurements: Modelling and experimental validation. Progress in Organic Coatings, 2021, 156, pp.106247. 10.1016/j.porgcoat.2021.106247 . hal-04030017

HAL Id: hal-04030017
https://hal.science/hal-04030017

Submitted on 24 Apr 2023

HAL is a multi-disciplinary open access archive for the deposit and dissemination of scientific research documents, whether they are published or not. The documents may come from teaching and research institutions in France or abroad, or from public or private research centers.

L'archive ouverte pluridisciplinaire **HAL**, est destinée au dépôt et à la diffusion de documents scientifiques de niveau recherche, publiés ou non, émanant des établissements d'enseignement et de recherche français ou étrangers, des laboratoires publics ou privés.

Distributed under a Creative Commons Attribution - NonCommercial 4.0 International License

Version of Record: https://www.sciencedirect.com/science/article/pii/S0300944021001181
Manuscript_641f9d4794b03d31506c21959c6dd549

BRDF and gloss computation of polyurethane coatings from roughness measurements: modelling and experimental validation.

B. Wittmann[a,c,*], P. Montmitonnet[a], A. Burr[a], C. Gauthier[b], J-F. Agassant[a], A. Casoli[c]

[a]MINES Paris, PSL* Research University, CEMEF, CNRS UMR 7635, Sophia Antipolis, 06904, France
[b]Université de Strasbourg, CNRS, Institut Charles Sadron UPR22, F-67000 Strasbourg, France
[c]Tarkett R&D Center Z.A. Salzbaach , L-9559, Wiltz, Luxembourg
[*]wittmannbenoit@gmail.com

Abstract:
Polyurethane coatings applied on PVC flooring substrate may influence its optical properties, especially gloss. Basically, rough surfaces look matte while smooth ones look glossy. However, the quantitative link between roughness and gloss remains insufficiently modelled. In this article, a microfacet-based model which predicts the BRDF from the 3D roughness slope distribution function f(dz/dx,dz/dy) is developed. Contrary to the different models existing in the literature, the computations are based directly on measured roughness from which the local slope distribution function is extracted. The model is applied to eight polyurethane coatings with different roughness and gloss. The results of the computations are compared to BRDF and gloss measurements. It is shown that this approach allows a good prediction of optical properties. In particular, the model predicts remarkably well the measured 60° gloss values.

Key words: Gloss, BRDF, coating, polymers

© 2021 published by Elsevier. This manuscript is made available under the CC BY NC user license
https://creativecommons.org/licenses/by-nc/4.0/

1. Introduction

Visual aspect is a key problem for all manufacturing industries, in particular surface finishing sectors. Among them, the flooring industry has to deal with multiple constraints. Indeed, the ambience of a room is directly linked to the design of the materials that compose the walls, the ceiling, and the floor. Different parameters have an influence on the visual aspect of materials: color, texture, transparency and, the aim of this article: gloss. The surface aspect must keep stable in time in spite of unavoidable wear, which changes the surface roughness. The question of the relationship between roughness and gloss is therefore crucial.

Gloss can be defined as the quantity of light reflected by a surface in the specular direction [1,2]. It is often measured thanks to a glossmeter, with a normalized method [3]. In many papers, authors try to link the roughness of materials to their gloss. Indeed, when a surface is smooth, it appears glossy, while it looks matte when rough [4]. By a physical optics approach, H.E. Bennett and J.O. Porteus [5] as well as P. Beckmann and A. Spizzichino [6] established a first link between roughness and gloss. T.E. Fletcher [7], M. Yonehara et al. [8] and I. Arino et al. [9] came to the same conclusion with empirical approaches: the gloss is a decreasing function of the arithmetical mean roughness ''R_a''. While very interesting on the practical level, these empirical approaches do not allow a fundamental understanding of the way roughness scatters light.

While gloss has the advantage to be fast and easily measured, it often gives results which do not correspond to the visual perception. For some authors, this difference comes from the fact that perception of gloss is a multi-dimensional phenomenon, and only one scalar is insufficient to describe it properly [10,11,12]. A more complete description of gloss can be obtained from the Bidirectional Reflectance Distribution Function (BRDF) measurement. The BRDF is defined as the ratio between the reflected radiance L_r and the incident irradiance E_i. It describes the way an incident light is reflected into space by a surface [13]. It contains, therefore, more information than the single scalar value given by a glossmeter [14,15]. Experimentally, this function is measured by goniospectrophotometry. Although this measurement is very rich, it is time-consuming because all the space directions must be scanned. This function is often measured in the literature to study the optical properties of materials (hair [16], leaves [17,18], tinfoil [19], glass [20], skin [21] …).

In 1967, Torrance and Sparrow [22] proposed a method to compute the BRDF from the surface roughness. The surface is modelled as a succession of microfacets following the laws of geometrical optics: each microfacet, which by hypothesis behaves like a mirror, has its own orientation, and reflects light in its specular direction. This involves a distribution function of the normal to the facets and a shadowing coefficient [23]. Then, numerous models based on this idea have been proposed, with different forms of the distribution function of the normal to the facets and of the shadowing coefficient. For example Oren and Nayar [24] describe each facet as a Lambertian diffuser, Ward [25] includes an anisotropic distribution function of the normal to the facets, Heitz et al. [26] use the Smith model to take into account the multiple reflections between the facets, D. Meneveaux et al. generalize this approach to a wide range of materials [27].

Generally, these microfacet models use Gaussian [22,24], Lorentzian [28] or Beckmann and Spizzichino [6,29,30] distribution functions of the normals to the facets. Walter et al. [31] compare these different distribution functions and propose a new one called ''GGX '' which has been used for example in [32]. M. Ribardière et al. [33] show the importance of the choice

of the distribution function of the normal to the facets on the rendering of computer-generated images.

In most studies, BRDFs models are successfully developed, to create realistic synthesis images for video games or special effects in movies for example. Here, the objective is some way the opposite: we want to understand the visual aspect of our floor covering material. For that purpose, a BRDF model is developed to link quantitatively the roughness of our materials to the way they scatter light.

These PVC flooring materials are coated with a thin polyurethane layer which aim is to improve the tribological properties of the material, as shown by Wittmann et al. [34]. However, as this coating constitutes the top layer of the material, it governs its gloss too. To control gloss, filler particles are added in the polyurethane formulation. These particles, the size of which is of the same order of magnitude as the coating thickness, more precisely 5-20 µm, create a micro-roughness which governs the gloss of the material. Conversely, their refractive index matches the one of the resin so that no volume diffusion is introduced. Therefore, the filler influences only surface properties, namely roughness and reflection. In practice, controlling the gloss from the formulation remains difficult and is always done by a trial and error approach.

The coating itself is very smooth, only the peaks corresponding to the filler particles emerge from it. The contribution of wavelength below the light wavelength is therefore very weak, so that diffraction effects are neglected hereafter.

In the present paper, a microfacet-based BRDF model calculated directly from roughness measurement is proposed. Eight PVC samples coated by filled polyurethane have been used to validate the approach. The kind of filler and their proportion in the coating formulation differ for each sample in order to get a wide range of roughness and gloss. The paper reports 3D roughness measurements of these eight materials by confocal rugosimetry. From these roughness measurements, the 3D slope distribution functions are computed, from which the BRDF is deduced. Then, the results given by the model are compared to experimental BRDF measured by goniospectrophotometry and gloss measurements.

This model has different objectives:

- Establishing an efficient BRDF determination from a simple roughness measurement thanks to a microfacet based model.

- Using this tool to interpret the visual aspects of real materials, based on their roughness.

- Understanding relationships between the coating roughness and its gloss in order to a priori tune the roughness geometry of a flooring for a targeted gloss.

2. Materials and methods

2.1. Samples studied

Each sample is a multi-layer material composed, from the bottom to the top, of: 2 mm of opaque PVC, black ink, 600 µm of transparent PVC, and a 20 µm polyurethane coating, as shown in Figure 1.

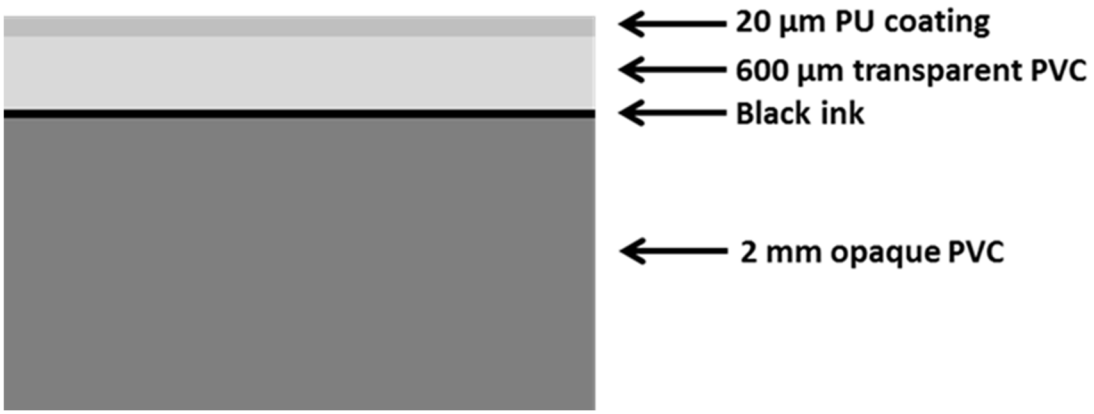

Figure 1 : Structure of the material.

The black ink layer is introduced in order to absorb, rather than reflect, the light that crosses the transparent PVC and PU. The coating is an acrylic UV cross-linked coating with a refractive index of 1.55, filled with particles that create a micro-roughness at the surface. The particles have a refractive index close to the one of the PU, so there is no volume light diffusion and the coating remains transparent. Eight samples are prepared, all with the same PU matrix, but with different kinds of fillers, with different particle sizes, and in different proportions in order to get a large range of roughness (Table I). Sample 8 has been obtained with specific crosslinking conditions, creating a particular roughness and serving as a very matte reference.

Table I shows that there is no simple relationship between the arithmetical mean rouchness Ra, the size of the particles, their proportion, and the gloss. This will be discussed in detail in section 5.1.

Table 1 : Samples prepared

Sample	**Fillers composition**	**Filler size**	**Weight proportion of filler**	**Ra (nm)**	**Gloss at 60° (GU)**
1	No filler	N/A	N/A	30	92
2	Silica	8 µm	10 %	150	35
3	Silica	5 µm	5 %	230	58
4	Silica	5 µm	10 %	250	26
5	Polyurea	7 µm	10 %	400	42
6	Polyamide	20 µm	10 %	460	75
7	Mix of particles	5-20 µm	10 %	480	29
8	No fillers	N/A	N/A	1800	2.5

2.2. Roughness measurements

The roughness of the different materials has been measured by a STIL chromatic confocal sensor (STIL SAS, Aix-en-Provence, France), with a MG210 optical pen (-x, -y resolution = 1 µm; -z resolution = 3 nm; maximum light cone angle = 43°). The measurements have been done on areas of 1 mm × 1 mm, with a -x and -y step of 1 µm.

2.3. Goniospectrophotometry

The apparatus shown on Figure 2 is a commercial spectrophotometer mounted on a home-made goniometric arm. It allows the measurement of the light diffusion profile (BRDF) of a material in the specular plane only, as described in detail in [35]. Furthermore, it is composed by:

- a 200W halogen-tungsten lamp positioned on a mechanical arm, allowing the control of the light incident angle on the sample from 0° to 85°. The beam is slightly divergent with a cone angle of 6°. With a normal incidence, the lit spot is a disc of 5 mm diameter much higher than the characteristic roughness asperities size (see appendix A), thus allowing an averaging on a large enough zone.

- a spectro-colorimeter (Ruby, STIL) positioned on another mechanical arm facing up the first one, allowing sweeping the reflection angle from 0° to 70°. It measures the relative luminance (in percent) reported to the one measured on a mirror. The sensor has an opening angle of 6°, meaning that it integrates the light on this angular range.

The apparatus does not have an azimuthal degree of freedom, meaning that measurements are not possible out of the specular plane.

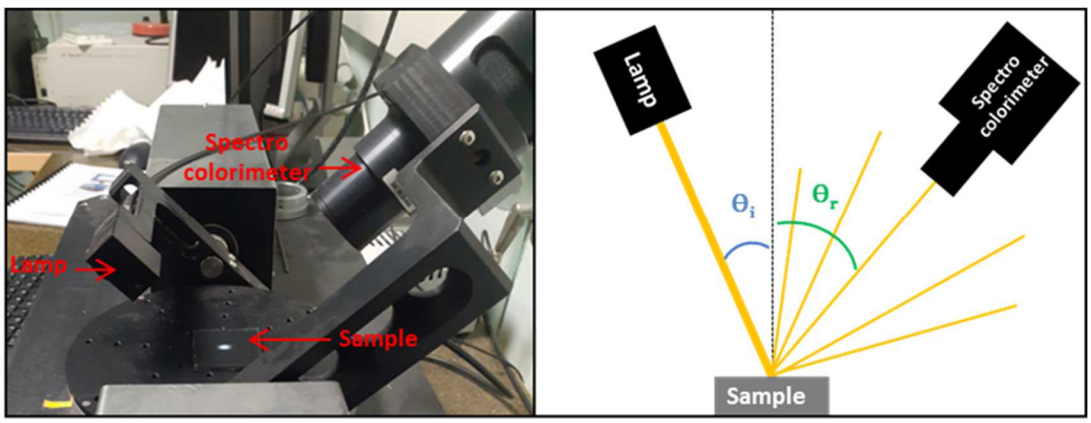

Figure 2 : Photograph and scheme of the goniospectrophotometer.

2.4. Glossmeter

Gloss measurements have been performed with a Micro-tri-gloss BYK. This apparatus follows the norm ISO 2813 [3]. The first measurements presented here are done with an incidence angle of 60°. In this configuration, the sensor has an aperture of 4.4° in the

measuring plane, and 11.7° in the perpendicular plane. The second measurements are done with an incidence angle of 85°. In this configuration, the sensor has an aperture of 4.0° in the measuring plane, and 6.0° in the perpendicular plane.

3. The BRDF model

The successive steps of the model are explained in detail and illustrated on sample 5.

3.1. Slope distribution function measurement

First, a roughness measurement is carried out on the surface of the material (Figure 3.a). This roughness measurement is differentiated with respect to both x and y to get the local slope of the surface in these two directions at each point. The local slopes in the –x and –y directions are computed respectively as (z(x+1µm)-z(x))/1µm and (z(y+1µm)-z(y))/1µm. Then, the discrete distribution ρ of these slopes is computed (Figure 3.b) with a step of 1.10^{-3} in the dz/dx and dz/dy directions. A cross-section of ρ, for dz/dx = 0 is shown in Figure 3.c. This discrete distribution will be used to compute the whole 3D BRDF.

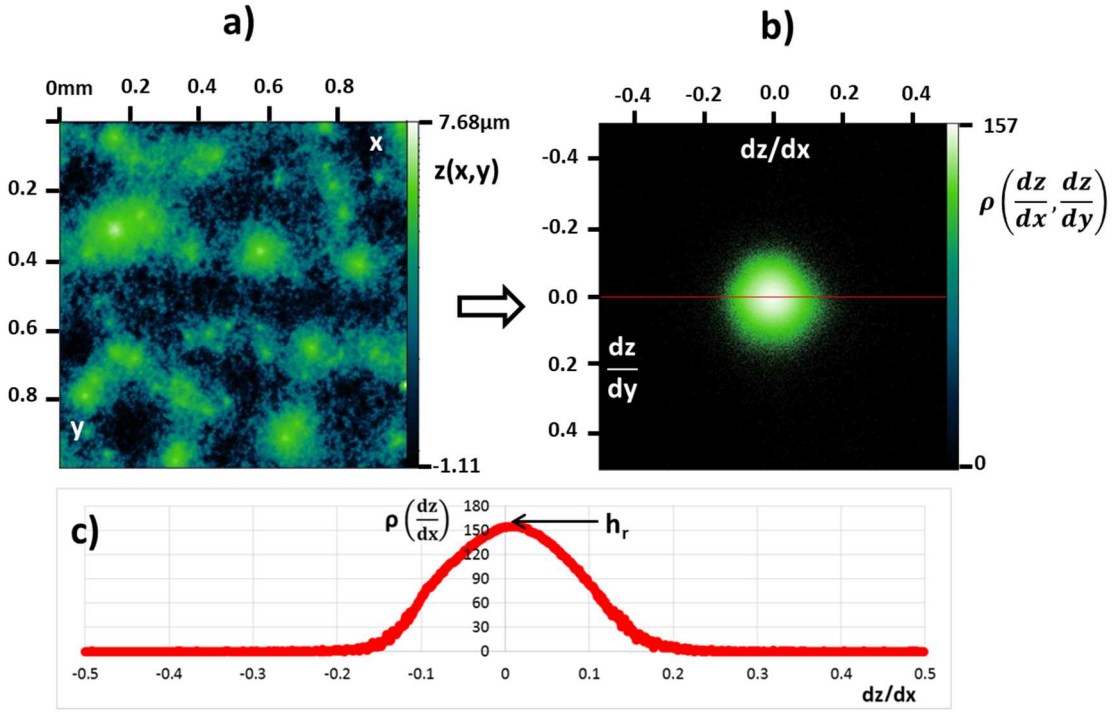

Figure 3 : Roughness height measurement of sample 5 (a), its slope distribution (b) and a cut of this slope distribution for dz/dx = 0 (c).

3.2. Reflection by a facet

We consider the 3 directing vectors in spherical coordinates (see figure 4):

-The incident direction I.

- The reflected direction R.

- The direction of the normal to a facet N.

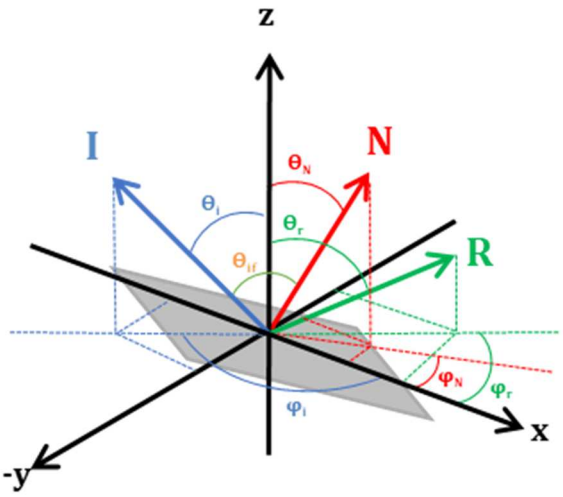

Figure 4 : Incident, normal and reflected vectors on a microfacet.

$$I=\begin{pmatrix}\theta_i\\ \varphi_i\\ 1\end{pmatrix} \qquad N=\begin{pmatrix}\theta_N\\ \varphi_N\\ 1\end{pmatrix} \qquad R=\begin{pmatrix}\theta_r\\ \varphi_r\\ 1\end{pmatrix} \qquad (1)$$

θ_k and φ_k (k=i,N,r) are respectively the zenithal and the azimuthal angles of the vectors I, N and R. The number "1" in the last line corresponds to the norm of each vector (that we take unitary).

The same vectors, expressed in the cartesian frame are written:

$$I=\begin{pmatrix}x_i\\ y_i\\ z_i\end{pmatrix} \qquad N=\begin{pmatrix}x_N\\ y_N\\ z_N\end{pmatrix} \qquad R=\begin{pmatrix}x_r\\ y_r\\ z_r\end{pmatrix} \qquad (2)$$

With $x_k=\sin(\theta_k)\cos(\varphi_k)$, $y_k=\sin(\theta_k)\sin(\varphi_k)$ and $z_k=\cos(\theta_k)$ (k=i,N,r)

The measure gives a slope distribution. However, the direction of the normal to the facet is here of interest. The plane equation for a facet can be written as:

$$-\frac{dz}{dx} \text{ x } -\frac{dz}{dy} \text{ y} + \text{z} = 0 \tag{3}$$

Therefore, once normalized (||N||=1), the N vector can be written in the cartesian frame:

$$N = \frac{1}{\sqrt{1+\left(-\frac{dz}{dx}\right)^2+\left(-\frac{dz}{dy}\right)^2}} \begin{pmatrix} -\frac{dz}{dx} \\ -\frac{dz}{dy} \\ 1 \end{pmatrix} \tag{4}$$

Geometrically, the vector R (reflected beam) is the symmetric of the vector I (incident beam) in relation to the axis directed by the normal N (in the plane defined by I and N).
Mathematically, this can be expressed as:

$$R = MI \tag{5}$$

With M the matrix of rotation of angle 180° around the vector N:

$$\text{M}=\begin{pmatrix} -1+2x_N^2 & 2x_Ny_N & 2x_Nz_N \\ 2x_Ny_N & -1+2y_N^2 & 2y_Nz_N \\ 2x_Nz_N & 2y_Nz_N & -1+2z_N^2 \end{pmatrix} \tag{6}$$

In spherical coordinates, we get:

$$\theta_r = \arccos(z_r)$$
$$\varphi_r = \begin{cases} \arccos\left(\frac{x_r}{\sqrt{x_r^2+y_r^2}}\right), & \text{if } y_r \geq 0 \\ 360 - \arccos\left(\frac{x_r}{\sqrt{x_r^2+y_r^2}}\right), & y_r < 0 \end{cases} \tag{7}$$

With

$$\begin{aligned} x_r &= \left(-1+2x_N^2\right)x_i + \left(2x_N y_N\right)y_i + \left(2x_N z_N\right)z_i \\ y_r &= \left(2x_N y_N\right)x_i + \left(-1+2y_N^2\right)y_i + \left(2y_N z_N\right)z_i \\ z_r &= \left(2x_N z_N\right)x_i + \left(2y_N z_N\right)y_i + \left(-1+2z_N^2\right)z_i \end{aligned} \quad (8)$$

Thanks to these relations, we can compute the reflected direction from the incident direction and the normal to the facet.

3.3. Proportion of light reflected by a facet

For dielectric materials (e.g. polymers), the fraction of light reflected by a facet depends on the refractive index of the material and the light incidence angle on the facet. This fraction is given by the Fresnel reflection coefficient [36]:

$$r\left(\theta_{if}\right) = \frac{1}{2}\left(\frac{\tan^2(\tau-\theta_{if})}{\tan^2(\tau+\theta_{if})} + \frac{\sin^2(\tau-\theta_{if})}{sin^2(\tau+\theta_{if})}\right) \quad (9)$$

With $\sin(\tau) = \frac{\sin(\theta_{if})}{n}$ where n in the refractive index of the material. In the case of the polyurethane studied here, n=1.55 . It has been evaluated thanks to a glossmeter measurement realised on the smooth sample 1. θ_{if} is the incident angle of the light on a facet (see Figure 4). As θ_{if} is the angle between the vectors I (incident light beam) and N (normal to the facet):

$$\theta_{if} = \left(\widehat{I,N}\right) = \arccos\left(\sin(\theta_i)\sin(\theta_r)\cos\left(\varphi_i-\varphi_r\right) + \cos(\theta_i)\cos(\theta_r)\right) \quad (10)$$

3.4. BRDF computation

For a given incident direction and a facet orientation, we can compute the reflected direction (equation 7). Moreover, we have a distribution of the facets orientations extracted from the roughness measurement (Figure 3.b) and the proportion of light that is reflected by a facet (equation 9). Therefore, we can compute the BRDF. The result, for sample 5, for an incident direction of ($\theta_i = 45°$, $\varphi_i = 0°$) is plotted on Figure 5.

The computation is fast (<30s) because it is only proportional to the number of facets N_f.

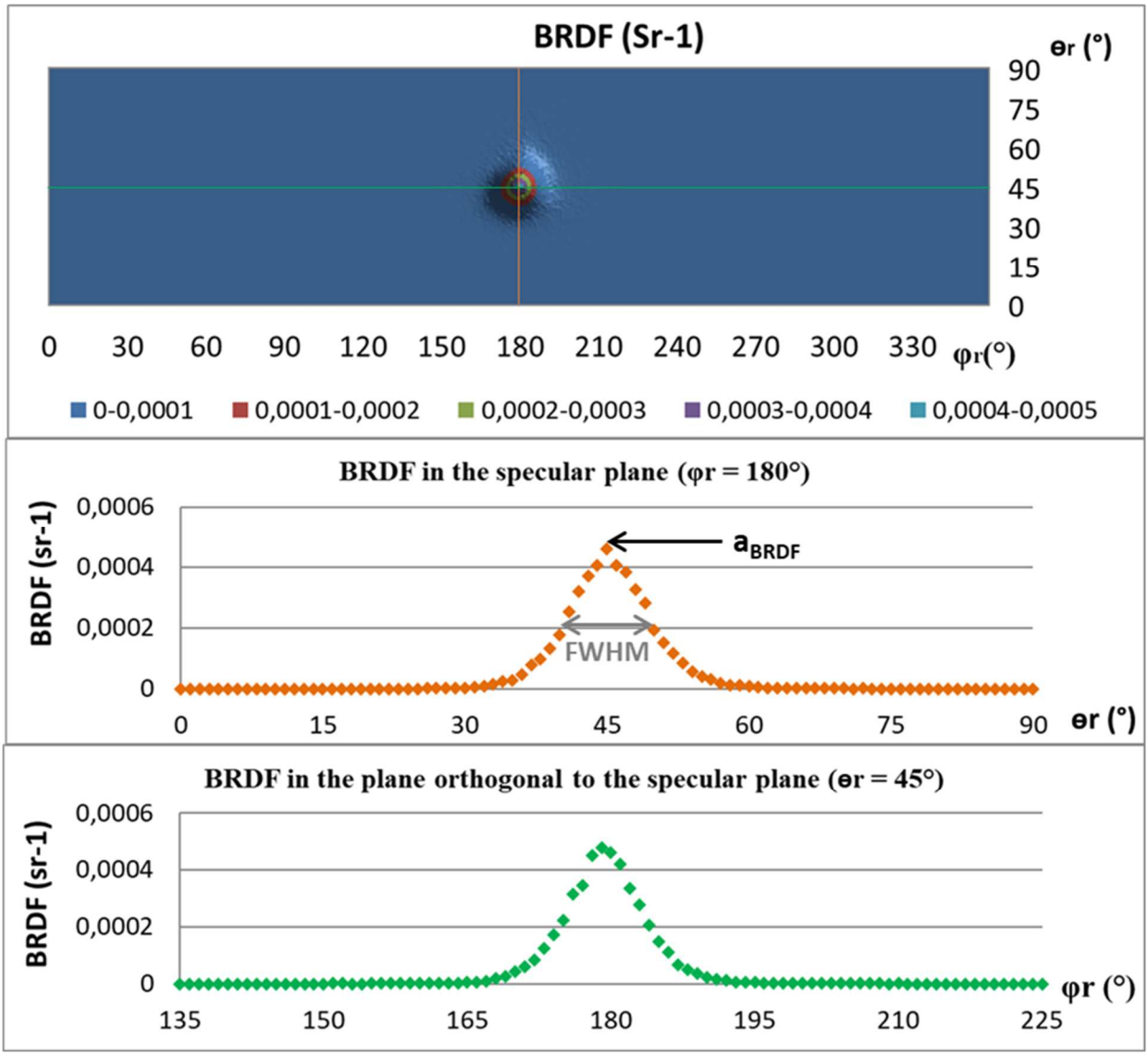

Figure 5 : BRDF computed for sample 5 with an increment of 1°. 3D BRDF (a), cross-section in the specular plane (b), cross-section in the plane orthogonal to the specular plane which contains the specular direction (c). The colours of symbols in b) and c) correspond to the colours of the cutting planes in a).

3.5. Correlation of the computation to the BRDF and gloss measurements

As the BRDF (unit: inverse of steradian, sr^{-1}) is a distribution function, it does not give an absolute value, but a proportion. Therefore, to correlate computations to measurements, the computed BRDF must be integrated over a given domain which depends on the measurement apparatus geometry. The way this integration was done, for the goniospectrophotometer and for the glossmeter, will be detailed in section 4.2 and 4.3.

4. Results

4.1. BRDF computations

A BRDF has been computed for each sample of Table 1 from their roughness measurements. All the roughness maps and their slope distributions are presented in appendix A. Each computation is done with $\theta_i = 45°$, $\varphi_i = 0°$ and n=1.55. $\theta i = 45°$ has been chosen just as an example as the middle of the interval [0°;90°]. On the other hand, $\varphi i = 0°$ has no importance as our surfaces are isotropic (cf the slope distribution functions in appendix A). Of course, if the studied surfaces were anisotropic, the choice of φi would be discussed. To visualize the influence of the roughness slope distribution on the BRDF, the amplitude of the computed BRDF a_{BRDF} (defined in Figure 5.b) is plotted as a function of the height of the roughness slope distribution function h_r (defined in Figure 3.c) in Figure 6.a. In Figure 6.b, the Full Width at Half Maximum ($FWHM_{BRDF}$) of the BRDF in the specular plane is plotted as a function of the height of the roughness slope distribution function.

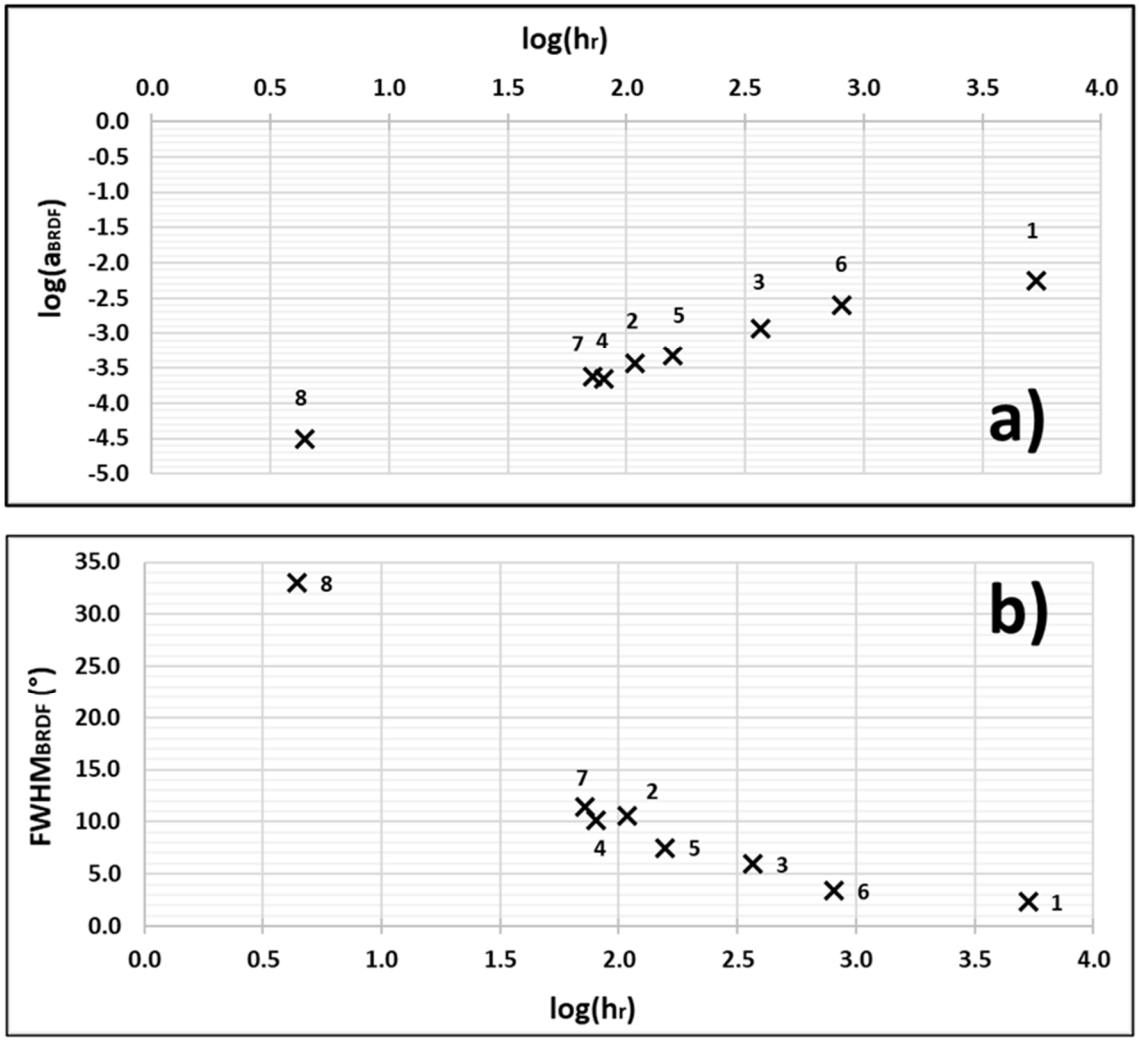

Figure 6 : Amplitude (a) and width (b) of the BRDFs as a function of the height of the roughness slope distribution function.

As explained by Seve [10], these two parameters (amplitude and width of the BRDF) are correlated with visual perception of gloss. Indeed, the amplitude of the BRDF corresponds to the glare of the sample while its width is correlated to the distinctness of the reflection (the wider, the less distinct).

Figure 6.a shows that the amplitude of the BRDF is a monotonically increasing function of the height of the roughness slope distribution function: a narrow slope distribution function (i.e. a sharp distribution) leads to a slender BRDF and vice versa. The width of the BRDF in the specular plane is a decreasing function of the height of the roughness slope distribution function: a sharp roughness slope distribution function (smooth sample) leads to a thin BRDF in the specular plane, and vice versa.

Note that the correlation is given here with the height of the slope distributions and not with Ra, although samples are numbered by increasing order of Ra (see Table 1). The reason why the present BRDF correlation with slope distribution is better than with Ra will be discussed in section 5.1**.**

4.2. Goniospectrophotometer measurements

In order to experimentally support the computations presented in section 4.1, BRDF measurements have been performed on each sample presented in Table 1. L is the relative luminance in percent of the one that would be obtained on a mirror. Each measurement, repeated 5 times, was done with $\theta_i = 45°$. One whole curve for samples 1 (glossy), 3 (semi-glossy) and 8 (matte) is presented on Figure 7.

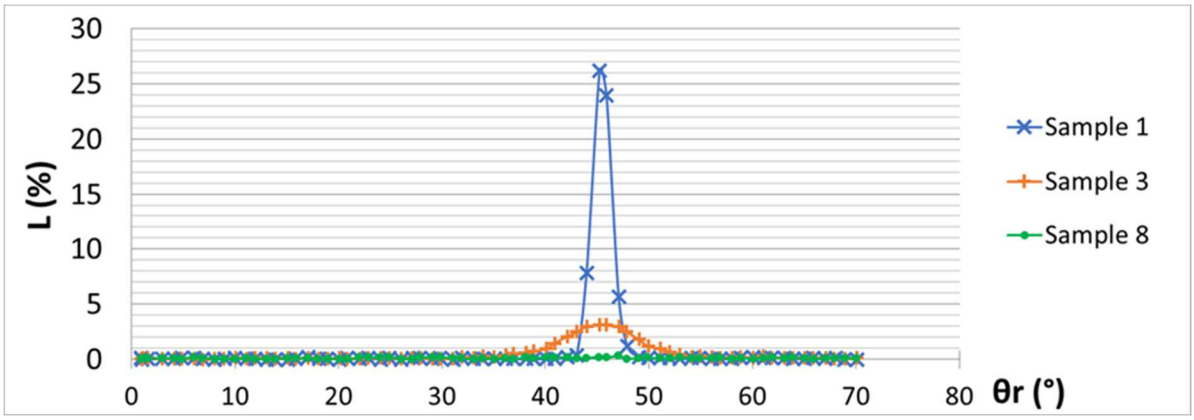

Figure 7 : BRDFs of the samples 1 (glossy), 3 (semi -glossy) and 8 (mat) in the specular plane, measured by goniospectrophotometry.

The glossy sample 1 has a high and thin BRDF. The semi-glossy sample 3 has a lower and wider one, meaning more diffusion. The sample 8, which is very matte, has a flat BRDF: the light is diffused by the surface roughness almost uniformly in all directions.

The amplitude and width of the BRDF measured for each sample are plotted respectively on Figure 8.a and Figure 8.b.

In order to compare quantitatively experimental to modelling results, one needs to integrate the computed BRDF on a 6° angle (the opening of the sensor) around each reflected direction

and multiply it by 100 to get a relative luminance in percent of the one that would be computed on a mirror. These modelling results are compared to the experimental ones on Figure 8.

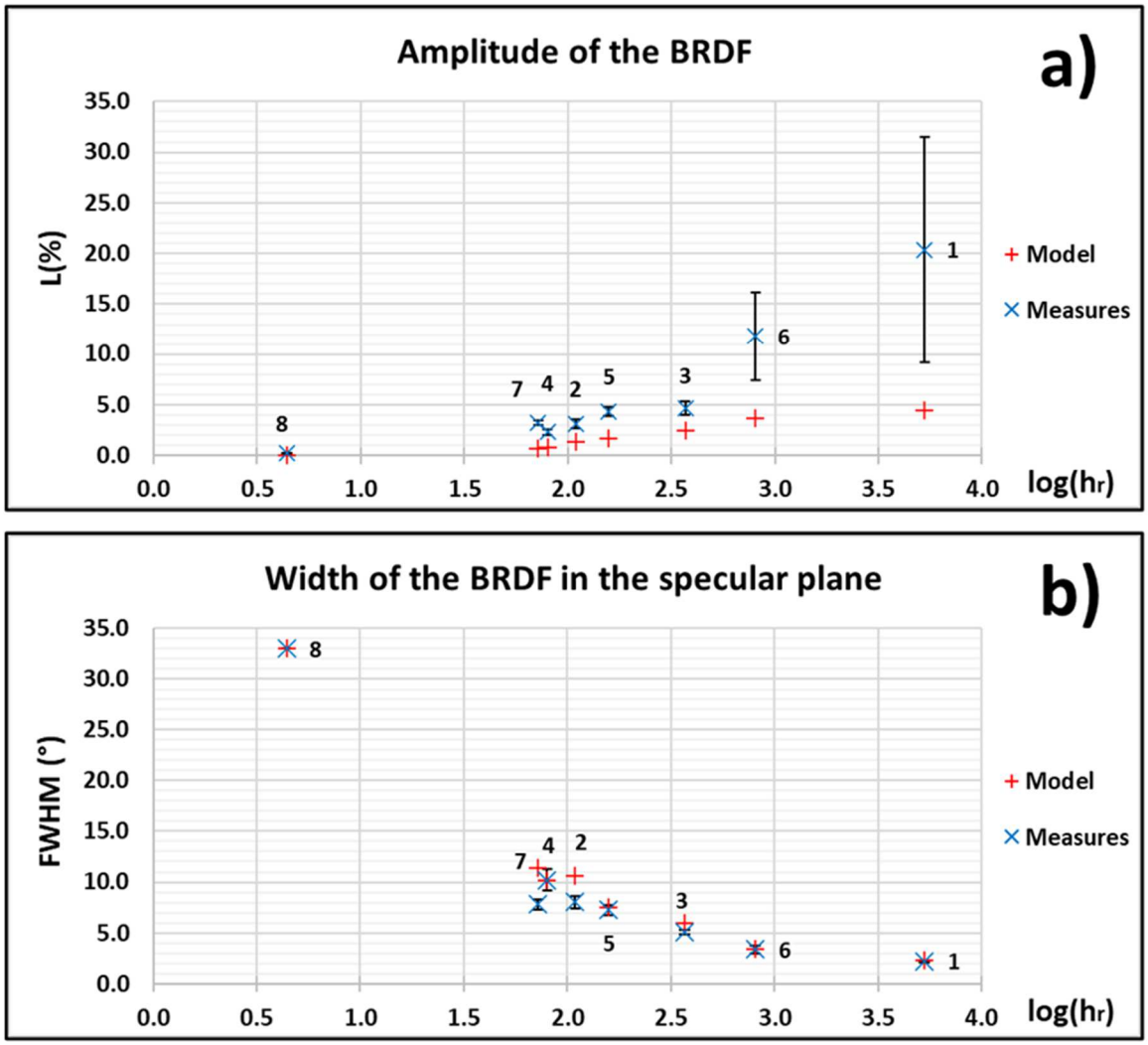

Figure 8 : Comparison between the model and experimental results: amplitude (a) and width (b) of the BRDF. Error bars represent the dispersion of 5 samples.

Amplitude of the BRDF: qualitatively, the experimental and modelling results are consistent. The amplitude of the BRDF is an increasing function of the height of the roughness slope distribution function. However, the model underestimates the experimental values. We also note a high dispersion of the measurements for the glossier samples. This dispersion is much lower for matte ones. An explanation is proposed in section 5.2**.**

Width of the BRDF: the computed widths fit very well the measured ones. Moreover, the dispersion of measured widths is very low.

4.3. Glossmeter measurements

This BRDF model can be used to compute the gloss of the samples. According to the norm ISO 2813 [3], gloss is the ratio between the flux measured on the sample in the specular

direction to the flux measured in the same conditions on a reference polished black glass with a refractive index n_{ref} = 1.567. In other words, for a given incident angle, the gloss expressed in gloss units (GU) is given by:

$$G(\theta_i) = 100.\frac{\Phi_{sample}(\theta_i)}{\Phi_{reference}(\theta_i)} \tag{11}$$

As the reference is mirror-polished, the reflected light is not diffused but completely reflected in the specular direction. Then $\Phi_{reference}$ is given by the Fresnel reflection coefficient. On the other hand, Φ_{sample} corresponds to the integral of the BRDF on a domain which depends on the geometry of the sensor. For an incident angle $\theta_i = 60°$, the glossmeter sensor has an opening of 4.4° in the measurement plane and 11,7° in the perpendicular plane. On the other hand, for an incident angle $\theta_i = 85°$, the glossmeter sensor has an opening of 4.0° in the measurement plane and 6.0° in the perpendicular plane Therefore, the gloss at 60° and 85° are computed as:

$$G(60°) = 100.\frac{\int_{\theta_r=60°-2.2°}^{\theta_r=60°+2.2°}\int_{\varphi_r=180°-5.85°}^{\varphi_r=180°+5.85°} BRDF_{sample}(\theta_r,\varphi_r).d\varphi_r d\theta_r}{r(n=1.567,\theta_i=60°)} \tag{12}$$

$$G(85°) = 100.\frac{\int_{\theta_r=850°-2°}^{\theta_r=85°+2°}\int_{\varphi_r=180°-3°}^{\varphi_r=180°+3°} BRDF_{sample}(\theta_r,\varphi_r).d\varphi_r d\theta_r}{r(n=1.567,\theta_i=85°)} \tag{13}$$

The BRDF of the 8 samples presented on Table 1 have been computed from their roughness slope distribution function with $\varphi_i = 0°$ and n =1.55. First, with $\theta_i = 60°$, and then with $\theta_i = 85°$. Then, from these BRDF, the gloss of each sample at 60° and 85° are computed respectively from equation 12 and 13. These computation results and the measured gloss are plotted as a function of the height of the roughness slope distribution on Figure 9.

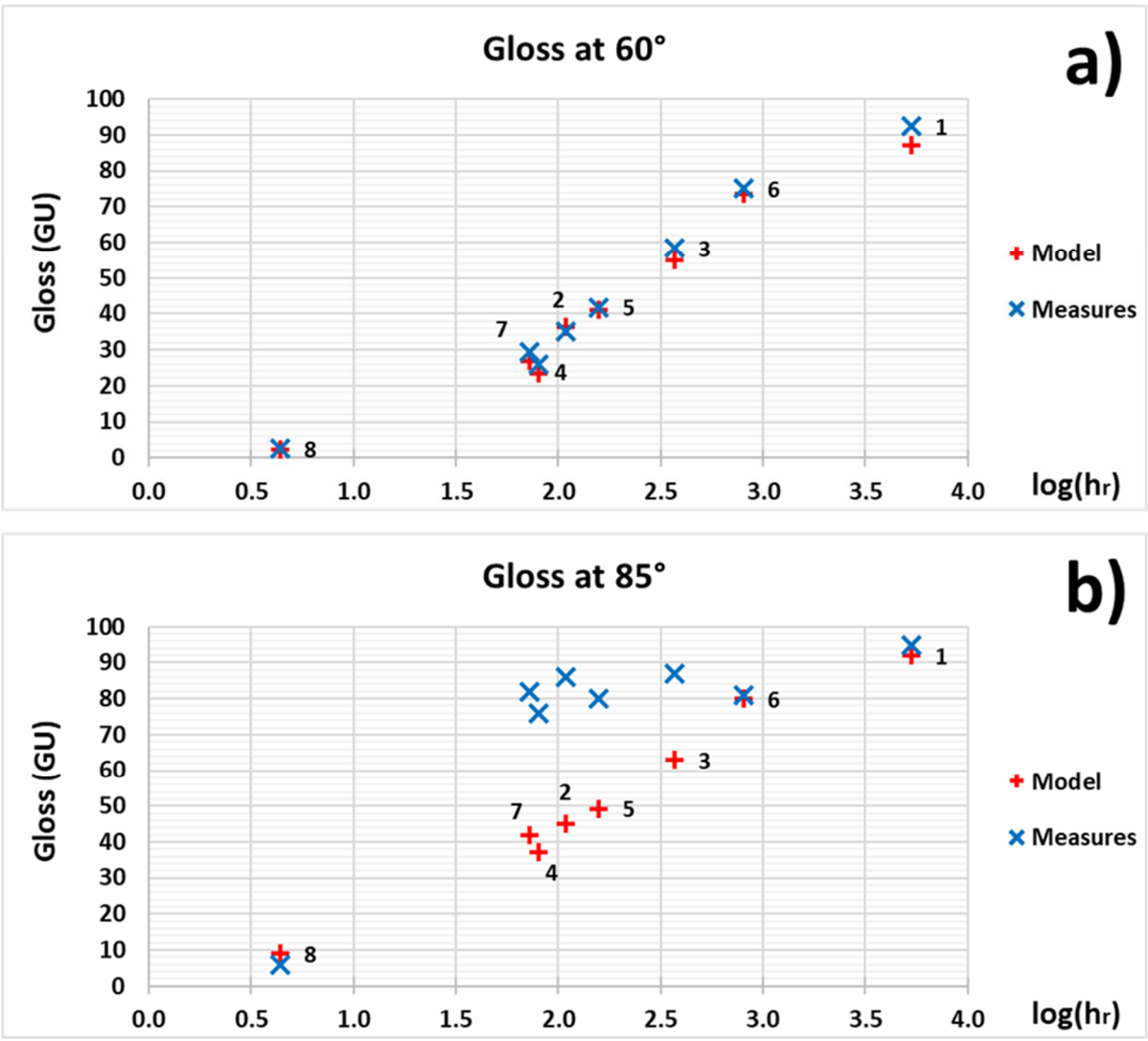

Figure 9 : Computed and measured gloss at (a) 60° and (b) 85° as a function of the height of the roughness slope distribution function.

For $\theta_i = 60°$, the computed gloss values correspond very well to the measured ones. Moreover, the gloss is an increasing function of the height of the roughness slope distribution function: high and thin slope distribution curve leads to high gloss and vice versa. This is consistent with the BRDF measurement results (section 4.2).

However, for $\theta_i = 85°$, the model is unable to predict the experimental values except for samples 1, 6 and 8. An explanation is proposed is section 5.4

5. Discussions

5.1. Relationships between roughness and gloss

The different results presented here show a very good correlation between the measured slope distribution function and the surface scattering properties, especially for gloss at 60°: the computed values accurately correspond to the measurements.

In the literature, it is often established [7,8,9] that the gloss decreases with the arithmetical mean roughness "Ra". In our case, we observe also this decreasing tendency, but the correlation is poor (see Figure 10).

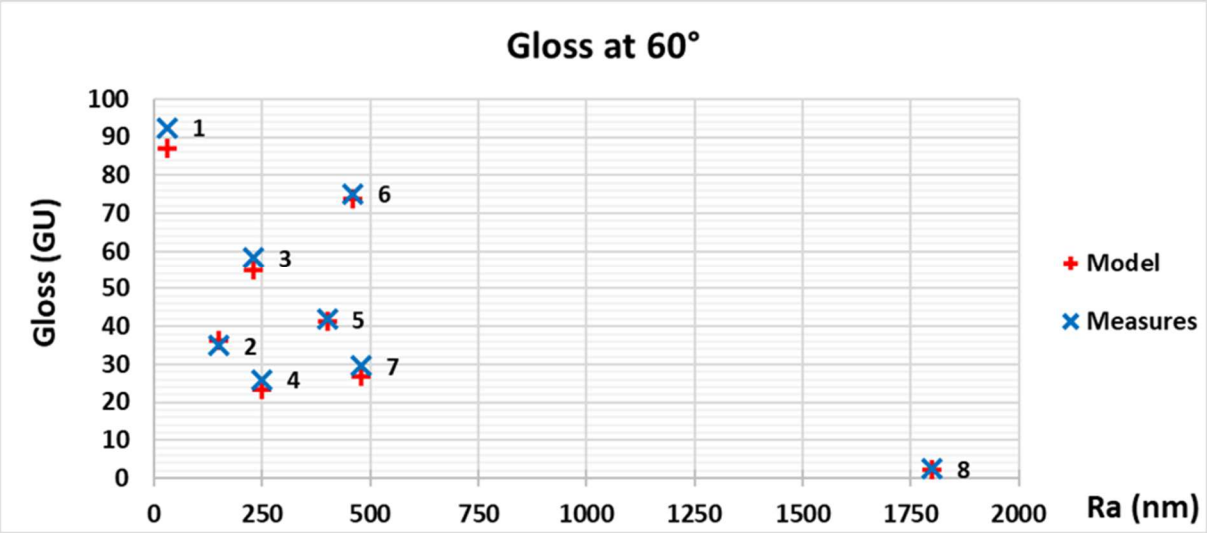

Figure 10 : Gloss at 60° as a function of the arithmetical mean roughness Ra.

This difference can be explained by the surface roughness geometry: when Ra is well correlated with gloss, all the samples have a similar roughness pattern geometry. For example, Fletcher [7] prepares polyurethane coatings filled with different kinds of silica particles, and in different concentrations, creating different levels of roughness. He shows that the correlation between Ra and gloss is very good for a given kind of particle (in different concentrations), but this correlation changes when the kind of filler is modified.

In the present paper, a large panel of fillers has been used. By changing the kind of filler, not only the Ra is modified but also the roughness geometry. For example samples 5 and 6, which have a close Ra, have a very different roughness geometry (see appendix A) leading to a big difference in gloss, just because polyurea (7 µm) has been replaced by polyamide (20 µm) without Ra change. In other words, Ra is sufficient to compare gloss of similar samples, but is insufficient for very different ones.

Conversely, the local slope-based model presented here seems to be general enough to link roughness to gloss (and BRDF) regardless of the roughness geometry differences between the samples. From our knowledge, it is the first time that this approach is proposed. We show that the absolute height of the slope distribution function h_r is a very relevant roughness parameter to interpret quantitatively differences in scattering properties.

5.2. Dispersion on the BRDF measurements

Figure 8.a shows a high dispersion on the amplitude of the BRDF for glossy samples while this dispersion is low for matte ones.

For glossy samples, the BRDF is localized and very thin. Therefore, the slightest shift in the experiment (lamp and sensor not perfectly aligned, sample tilted…) distorts highly the measured luminance because the sensor is not exactly on the peak of the BRDF. On the other hand, matte samples have a wide and diffuse BRDF, so the value of the BRDF does not vary so much around the specular direction and the uncertainty on the measure is lower. This could explain why the dispersion of the measurements is higher on glossy samples. The latter require a very accurate sensor with a high resolution.

5.3. Underestimation of the BRDF amplitude

Figure 8.a shows that the model underestimates the values of the BRDF amplitude especially for glossy samples. All measured values are reported to the one made on a mirror. As explained in the previous section, the uncertainty on glossy samples is high. The mirror does not escape this rule. Therefore, if there is a slight shift between the light source and the sample (not perfectly aligned), the BRDF is measured slightly out of the mirror's BRDF peak and the value is underestimated. As a consequence, the values measured on the samples are overestimated. In this scenario the difference between the measured and computed BRDF values comes from an experimental shift.

5.4. Limits of the model

A first phenomenon that is not accounted for in this model is the shadowing/masking. Our approach consists in modelling the surface scattering in a statistical way: each facet having the same orientation is considered equivalent. To model shadowing and masking effects, one needs to account for the neighbourhood of each facet. In this context, two facets having the same orientation are not equivalent if their neighbourhood is different. Therefore, to model shadowing/masking effects, our statistical approach is not consistent anymore, one needs to use a more sophisticated approach, like ray tracing e.g. Another possibility would be to multiply our computed BRDF by a masking/shadowing coefficient. For example, Torrance and Sparrow [22] compute such a coefficient considering the surface as a succession of "V" cavities. Masking and shadowing effects are substantial when slopes of local roughness are high and light incidence is grazing [26].

The second phenomenon that is not considered here is multi-reflections. Indeed, with very high local slopes, it is possible that a reflected ray meets a second facet after being reflected by a first one. Again, the statistical approach does not allow this phenomenon because one needs to know the neighbourhood of each facet. Moreover, it is probable that this multi-reflection is totally negligible on polymeric materials. Indeed, most of the incident light is refracted in the bulk of the material and only a few percents is reflected. For the PU material having a refractive index n=1.55, only 8% of light is reflected with $\theta_i = 60°$ based on the Fresnel coefficient. Therefore, after a second reflection, only about $(0.08)^2=0.0064=0.64\%$ is reflected.

It is surprising to notice how much the model is able to predict the gloss at 60° (see figure 9.a) while it is not the case at 85° (see figure 9.b). One could think that the reason is that shadowing/masking effects are not negligible anymore at 85° which is a grazing angle. Actually, this interpretation does not work. Indeed, if it was right, the rougher samples would be the most impacted. However, we note that the model fits well the experimental measurement for sample 8 which is the roughest (see table 1). Another analyze, raising a deeper problem, could explain this difference: according to the incidence angle, the light does not "see" the roughness the same way. In order to illustrate this idea, we can consider the saw-tooth profile on figure 11.a. The roughness profile has a spatial period d. However, the incident light does not "see" the profile of the real roughness but its orthogonal projection on the plane perpendicular to the incidence direction (the red plane in the figure). In this way, the light "sees" a surface of period d', with:

$$d' = d.\cos(\theta_i) \qquad (14)$$

d' is plotted as a function of θ_i on figure 11.b for d=5µm. This corresponds roughly to the roughness of a coating filled with 5µm particles. d' is a decreasing function of the angle of incidence. With d = 5 µm, d'<800 nm for θ_i> 80, and this explains the observed discrepancies: if the spatial period of the roughness is less than the light wavelength, the facet model is no longer valid. The characteristic size of the asperities being "seen" by the light as lower than its wavelength, it interacts with the surface as if it were smooth. To account for this phenomenon, it would be necessary to use a physical optics model. These calculations on a saw-tooth geometry have not the pretension of being quantitative. They just illustrate that the facet model is no longer valid in very grazing incidence.

If the idea presented above is correct, the diffusion by roughness calculated by the model of facets should be overrated and this is what happens: if the diffusion is overvalued, the amplitude of BRDF and therefore gloss is underestimated. However, it is observed that the model corresponds well to the measurements for samples 1 and 6 with the thinner distribution of slopes (see appendix A). This also supports the explanation mentioned above: if the surface is smooth, the geometry of the surface and its projection on the plane perpendicular to the direction of incidence are identical, and therefore the effect of projection has no influence. Surprisingly, we note also that the calculation on sample 9 corresponds well to measure. This is the roughest sample, but with a very particular roughness geometry (in the form of beads, having a characteristic size of the order of 10 µm, see appendix A). In this specific case, the characteristic roughness size (parameter d in Figure 11.a) is large enough so that d' is always greater than 800 nm at an incidence of 85° and the facet model is still applicable.

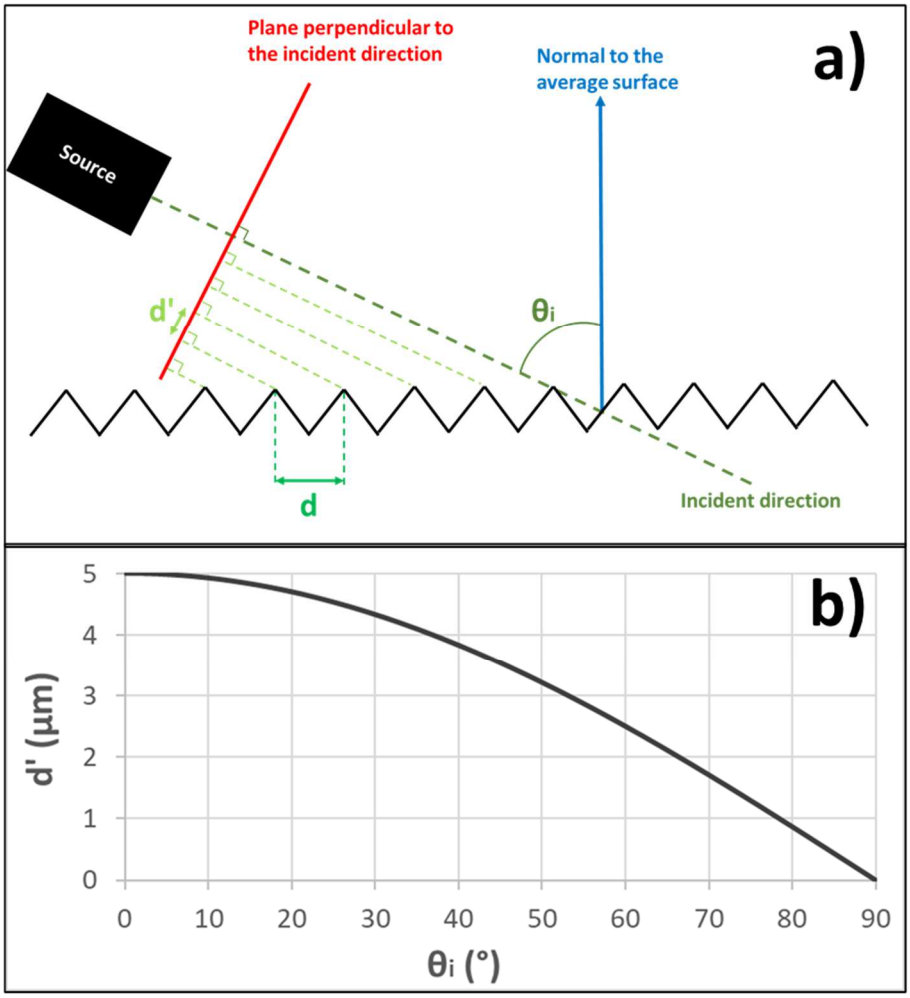

Figure 11: (a) Projection of a sawtooth roughness profile on the plane normal to the direction of incidence. (b) d' as a function of θ_i for d=5µm.

6. Conclusion

In this paper, a microfacet-based BRDF model is proposed. The novelty is to compute it directly from roughness measurements from which the local slope distribution function is extracted. This approach shows the potential of microfacet modelling when accurate information about surface roughness is available. This model has been applied to several polyurethane coatings with different roughness to compute their light scattering properties and gloss. It is shown that the model results broadly agree with the experimental ones. In particular, it remarkably well predicts gloss measurements for an incidence of 60°.

Moreover, it has been shown that the height of the roughness slope distribution function is a more adequate parameter than the arithmetical mean roughness Ra, it gives a much stronger correlation between roughness and gloss. This is due to the dominant physical interaction between the surface and light with the present range of roughness: specular reflection on microfacets clearly puts emphasis on the orientations of the normals. Other surface description parameters could be more interesting in other ranges of roughness or other physical properties.

In the practical problem of polyurethane coatings presented here, this tool can be used to adapt a formulation to a targeted gloss. Indeed, the good predictions it provides allow a good understanding of the link between the roughness (mainly brought by the filler) and the optical properties. Of course, qualitatively, all coating formulators know that increasing the roughness leads to decrease gloss. But the method and the model presented here allow linking quantitatively these two parameters. Often, it remains difficult for formulators to understand the way gloss evolves by modifying one component of the formulation (the size of the fillers for example) as long as the simple arithmetic roughness is not a sufficient parameter. Thanks to the method proposed here, one just needs to measure the roughness and apply the model to interpret the influence of some ingredients in the formulation on the final gloss of the material.

This model can also be used to address another important practical problem, the long-term evolution of the optical properties due to the different mar and wear modes. This work has been undertaken in the case of the visibility of scratches [37].

Funding

This study has been financed by the Tarkett company, as a part of an industrial PhD project.
The support of the French National Agency for Research and Technology (ANRT) is gratefully acknowledged (grant CIFRE 2017/0849).

References

[1] V.G.W. Harrison. Definition and measurement of gloss: a survey of published litterature. Printing and allied trades research association, Leatherhead, Surrey, Great Britain, 1945.

[2] V.G.W. Harrison, S.R.C. Poulter. Gloss measurement of papers - the effect of luminance factor. British journal of applied physics. 1951, Vol. 26, pp. 92 - 97.

[3] IOF STANDARDIZATION. ISO 2813. Paints and varnishes–determination of gloss value at 20 degrees, 60 degrees and 85 degrees. 2014

[4] S.E. Maskery. Development and applications for matting agents. Pigment & Resin Technology. 1973, Vol. 2, pp. 11-19.

[5] H.E. Bennett and J.O. Porteus. Relation Between Surface Roughness and Specular Reflectance at Normal Incidence. Journal of the optical society of America. 1961. Vol. 51, pp. 123-129

[6] P. Beckmann, A. Spizzichino. The scattering of electromagnetic waves from rough surfaces. Pergamon Press, Oxford, 1963

[7] T.E. Fletcher. A simple model to describe relationships between gloss behavior, matting agent concentration and the rheology of matted paints in coatings. Progress in organic coatings. 2002, Vol. 44, pp. 25 - 36.

[8] M. Yonehara, T. Matsui, K. Kihara, H. Isono, A. Kijima, T. Sugibayashi. Experimental relationships between surface roughness, glossiness and color of chromatic metals. Materials Transactions. 2004, Vol. 45, pp. 1027 - 1032.

[9] I. Arino, L. Mattson, M. Rigdahl. On the relation between surface texture and gloss of injection-molded pigmented plastics. Polymer engineering and science. 2005, Vol. 45, pp. 1343 - 1356.

[10] R. Sève. Problems connected with the perception of gloss. Color research and application. 1993, Vol. 18, pp. 241 - 252.

[11] J.A. Ferwerda, F. Pellacini, D.P. Greenberg. A psychophysically-based model of surface gloss perception. Proceedings of SPIE - The International Society for Optical Engineering. 2001, Vol. 4299, pp. 291 - 301.

[12] G. Ged, G. Obein, Z. Silvestri, J. Le Rohellec, F. Viénot. Recognizing real materials from their glossy appearance. Journal of vision. 2010, Vol. 10, pp. 1 - 17.

[13] C. Wynn. An introduction to BRDF-Based lighting. Nvidia corporation. 2000. https://www.cs.princeton.edu/courses/archive/fall06/cos526/tmp/wynn.pdf

[14] I. Nimeroff. Analysis of goniophotometric reflection curves. Journal of research of the national bureau of standards. 1952, Vol. 49, pp. 441 - 448.

[15] F. Leloup, P. Hanselaer, J. Versluys, S. Forment. BRDF and gloss measurements. Proc. CIE Expert Symp. Visual Appearance, Paris, 2006, CIE (Commission Internationale de l'Eclairage).

[16] C. Reich, C.R.Robbins. Light scattering shine measurements of human hair: a sensitive probe of the hair surface. Journal of the society of cosmetic chemists. 1993, Vol. 44, pp. 221-234.

[17] L. Bousquet, S. Lachérade, S. Jacquemond, I. Moya. Leaf BRDF measurements and model for specular and diffuse components differentiation. Remote sensing of environment. 2005, Vol. 98, pp. 201 - 211.

[18] A. Comar, F. Baret, F. Obein, L. Simonot, D. Meneveaux, F. Viénot, B. de Solan. A leaf BRDF model taking into account the azimuthal anisotropy of monocotyledonous leaf surface. 2014, Vol. 143, pp. 112-121.

[19] H. Wang, W. Zhang, A. Duong. Measurement and modeling of Bidirectional Reflectance Distribution Function (BRDF) on material surface. Measurement. 2013, Vol. 46, pp. 3654-3661.

[20] F.B. Leloup, M.R. Pointer, P. Dutré, P. Hanselaer. Luminance-based specular gloss characterization. Journal of optical society. 2011, Vol. 28, pp. 1322-1330.

[21] A. Sohaib, L. Broadbent, A.R. Farooq, L.N. Smith, M.L. Smith. BRDF of human skin in the visible spectrum. Sensor review. 2017, Vol. 37, pp. 390-395.

[22] K.E. Torrance, E.M. Sparrow. Theory of off-specular reflection from roughnes surfaces. Journal of the optical society of america. 1967, Vol. 57, pp. 1105 - 1114.

[23] E. Heitz. Understanding the masking-shadowing function in microfacets-based BRDFs. Journal of Computer Graphics Techniques. 2014, Vol. 3, pp. 48-107.

[24] M. Oren, S.K. Nayar. Generalization of Lambert's Reflectance model. SIGGRAPH '94: Proceedings of the 21st annual conference on Computer graphics and interactive techniques. 1994, pp. 239–246.

[25] G.J. Ward. Measuring and modeling anisotropic reflection. Computer graphics. 1992, Vol. 26, pp. 265 - 272.

[26] E. Heitz J. Hanika, E. d'Eon, C. Dachsbacher,. Multiple-Scattering microfacet BSDFs with the Smith model. ACM transactions on graphics. 2016, Vol. 35, pp. 1-14.

[27] D. Meneveaux, B. Bringier, E. Tauzia, M. Ribardière, L. Simonot. Rendering rough opaque materials with interfaced lambertian microfacets. IEEE transactions on visualization and computer graphics. 2017, Vol. 24, pp. 1368–1380.

[28] G. Obein, T. Leroux, F. Viénot. Bi-directional reflectance distribution factor and gloss scale. Human vision and electronic imaging. 2001, Vol. 4299, pp. 279 - 290.

[29] R.L. Cook, K.E. Torrance. A reflectance model for computer graphics. ACM Transactions on graphics. 1982, Vol. 1, pp. 7 - 24.

[30] C. Kelemen, L. Szirmay-Kalos. A microfacet based coupled specular-matte BRDF model with importance sampling. Eurographics. 2001.

[31] B. Walter, S.T. Marschner, H. Li, K.E. Torrance. Microfacet Models for Refraction through Rough Surfaces. Eurographics symposium on rendering. 2007.

[32] M. Ribardière, M. Bringier, D. Meneveaux, L. Simonot. STD : Student's t-distribution of slopes for microfacet based BSDFs. Computer graphics forum. 2017, Vol. 36, pp. 421-429.

[33] M. Ribardière, B. Bringier, L. Simonot, D. Meneveaux. Microfacet BSDFs generatef from NDFs and explicit microgeometry. ACM Transactions on graphics. 2019, Vol. 38, pp 1-15.

[34] B. Wittmann, C. Gauthier, A. Burr, J-F. Agassant, D. Favier, P. Montmitonnet, A. Casoli. Study of scratch resistance of a hard-on-soft polymer bilayer : combination of in-situ vision, X-ray tomography and numerical simulations. Wear. 2020, Vol. 452-453.

[35] B. Goffette. Couleurs de polymères chargés pour un environnement lumineux (in french) - Colors of charged polymers for a bright environment . PhD thesis, Mines ParisTech. 2013.

[36] L. Simonot, P.Boulenguez. Quand la matière diffuse la lumière (in french) - When matter diffuses light. Presse des mines, 2019.

[37] B. Wittmann. Matériaux et procédés de la micro- et macro- texturation de surface de revêtements de sols: propriétés optiques et tribologiques (in french) - Materials and processes of the micro and macro texturation of floor covering surfaces: optical and tribological properties. PhD thesis, Mines ParisTech. 2020.

Appendix A: Roughness measurements and their slope distribution.